Hydrogeochemical Facies Investigation of Surface and Groundwater Resources at West Luxor Area, Egypt, Using Spatial and Statistical Techniques

Mervat A. El-Sonbati[1], Maie I. El-Gammal[1], Ahmed M. El-Zeiny[2], Mohamed A. Gebril[3*]

[1] Environmental Science Department, Faculty of Sciences, Damietta University, Egypt
[2] Environmental Studies Department, National Authority for Remote Sensing and Space Sciences (NARSS), Egypt
[3] Geochemical studies Department, central laboratories, Egyptian Mineral Resources Authority (EMRA), Egypt

ABSTRACT

Water quality and quantity have diminished in the agricultural area of west Luxor due to excessive water use and land management techniques. The current study intends to monitor the hydrogeochemical processes of water resources in Egypt's west Luxor area. In August 2021, 79 surface, shallow, and groundwater samples were collected in the study area. In this investigation, three statistical techniques were used: classical, cluster hydrogeochemical statistical analysis (CA), and geo-statistical analysis. Water characteristics are mapped using the Kriging method, which is a Geo-Statistical tool in ArcMap 10.4.1. The laboratory results of the Piper trainer diagram integration (CA) and geo-statistical prediction maps showed that cations ($Na^+ > Ca^{2+} > Mg^{2+} > K^+$) and anions ($Cl^- > SO_4^{2-} > HCO_3^- > CO_3^{2-}$) dominated. The majority of water types in all samples were Na-Cl, Mixed Na-Cl-HCO$_3$, Mixed Na-Cl-SO$_4$, and Mixed Na-Ca-Mg-HCO$_3$. Prediction maps coincide with hydro-geochemical statistical analysis, which showed that salts and measured heavy metals (Fe, Mn, Co, Ni, Cd, Pb, As) levels in groundwater and shallow water samples were greater than those of Egyptian Standard Limits, while surface water had high pH, HCO$^-$, and CO$_3^{2-}$ levels, indicating pollution sources. As a result, this study found that combining geostatistical and classical hydrogeochemical statistical analysis produced a good assessment of both natural water processes and water quality in the west Luxor area.

Keywords: Geo-Statistical analysis; GIS; Hydrogeochemical investigations; Hydmorphometric parameters; Luxor hydrogeology

INTRODUCTION

The chemistry of water from different resources; surfaces, and shallow or deep groundwater results from the disintegration of solid minerals, precipitation of solids resulting from water-rock and water-soil interactions, sorption/ion exchange, and dissolution or evolution of gases. It helps to understand the hydrogeochemical process and its impacts on the environment and examine human impacts against natural conditions and the evolution of water quality (El Alfy *et al.*, 2018; Jamil, *et al.*, 2020). The variation in concentration of the different water-dissolved hydrogeochemical constituents determines its usefulness for domestic, industrial, and agricultural purposes (Zhang *et al.,* 2018; Xu *et al.*, 2019).

Cluster analysis (CA) is considered one of the chemometric methods, it is a useful method for combining water samples into homogenous groups according to their water quality. Results can be displayed as a tree diagram (dendrogram), which provides a visual summary of the clustering process through a helpful graphical tool for determining the number of clusters that describes the underlying process and finally lead to spatial variation. HCA supplies a complete analysis of information in organized formate and uses for the interpretation of hydrogeochemical processes by formulating hypotheses (Wu *et al.*, 2014; Deepesh *et al.,* 2015).

The spatial distribution of water quality shows some heterogeneity and the determination of quality parameters at the whole location is not always feasible under the time and cost of the data collection. Thus, the prediction of values based on selectively measured one is an alternative while minimizing errors and enhancing the rate of accurate calculation. Geographical Information System (GIS) is a leading tool that has great potential for use in problem-solving in various areas, including environmental fields (Mahato *et al.*, 2016; Çelik 2019). Geo-statistical tools fill up the gap between geo-statistics and GIS. The interpolation analysis of groundwater levels with geostatistical modules became easier and more operable with the development of GIS technology, which can characterize the spatial variability of parameters in more detail (Triki *et al.,* 2013; Bao *et al.,* 2014; Agarwal *et al.*, 2016).

Spatial interpolation is a procedure of predicting the value of attributes at un-sampled sites from measureements made at point locations within the same area. Several kinds of research have been accepted to compare different interpolation methods in a variety of situations, using GIS in different areas such as groundwater; depth, contamination, quality, etc., (Chai *et al.* 2011; Losser *et al.*, 2014; Xiao *et al.*, 2016). Geostatistical interpolation consists of ordinary Kriging (OK), simple Kriging (SK), and universal Kriging interpolation (UK). Deterministic interpolation comprises global polynomial (GPI), local polynomial (inverse distance weighted (IDW)), planar spline, and local polynomial interpolation (LPI) (Zandi *et al.*, 2011; Ahmadian and Chavoshian, 2012). The posterior method can be used to correct the local errors without reducing the accuracy, the precision of the method is close to the Kriging techniques (Gunarathna, *et al.*, 2016; Al-Omran *et al.*, 2017; Aslan and Çelik, 2021). A considerable amount of literature has been published on water quality in Egypt, including many topics such as water quality assessment and groundwater pollution (Sabry, *et al.,* 2019) but there were no reported

---

researches on the investigation and verification of hydrogeochemical processes of water resources using statistical techniques. Therefore, this study aims at integrating the geostatistical and statistical hydrogeochemical approaches to examine the regional factors and processes which control the chemical composition of water bodies; surface, shallow, and deep groundwater in the region of west Luxor.

MATERIALS AND METHODS

The flow chart of the methodology assumed to screen the hydrogeochemical processes of water resources and water quality mapping using water quality characteristics in the GIS environment is shown in Figure (1).

Study area

The study area is located on the west bank of the River Nile in Luxor Governorate, Egypt. It is extended between Latitudes 25° 8′ to 25° 55′ N and Longitudes 32° 11′ to 32° 44′ E (Figure 2). The area is distinguished by an arid climate with average maximum and minimum temperature ranges between 22.9 °C- 40.9 °C and 5.7 °C - 23.9 °C in January and July, respectively. The wind speed fluctuates spatially and temporarily with monthly average values of 5.9 km/h in October and 9.3 km/h in April. The relative humidity monthly average values vary between 25.0 % in May and 55.0 % in December. The monthly average precipitation ranges between 0.0 and 0.3 mm and falls randomly throughout the year (Salman *et al.*, 2019).

Topography of Luxor

Luxor government involves different topography as shown in Figure (2), at the entire Nile valley where there are agricultural activities and residential communities. New cultivated borders in the west with an extension of mountainous heights and sandy hills characterize the edges of the valley on the western flanks. (Abou Hussein and Sawan 2010; Ahmed and Fogg, 2014).

Geology of Luxor

The geological features and formations of the Luxor area (Figure 3) were digitized from the Geological map (CONOCO, 1987). Upper Cretaceous, Pliocene, Paleocene-Eocene, and Pleistocene-Holocene characterized the geology of the study area (Said, 1981; Kamel, 2004). The Pliocene unit is exemplified in the Luxor area by two formations namely: Pliocene fault breccia and the Madamud Formation. The Pleistocene unit comprises the Protonile, the Prenile, and the Neonile sediments of the Early, Middle, and Late Pleistocene ages, respectively. The Protonile sediments are presented by the Arment Formation. The Prenile sediments are represented by the Qena Formation, and the Abbassia Formation. The Holocene unit is signified by the Neonile sediments (Arkin Formation). The recent alluvial cover comprises unconsolidated sediments characterized by the Nile flood plain unit made up of two sequential layers (silty clay and clay layers) with a total thickness of 18.5 m (Ahmed and Fogg, 2014).

Hydrogeology of the study area

The Nile River and irrigation canals, particularly the two main canals, Asfun and Al-Kallabiyya, provide the hydrology of surface water for the studied area (Figure 2). At the Luxor area, two major groundwater aquifers were well characterised by Said (1981), Abd El-Bassier (1997) and Ahmed and Fogg, (2014) and their hydrogeological cross-section are shown in Figure (4): The Quaternary aquifer is the most prominent water-bearing structure in Luxor, occupying the centre stripe of the Nile Valley and forming the historic cultivated areas on both Nile sides. The lower Pleistocene aquifer and the higher Holocene aquitard are the two hydrogeological units. The Pliocene-Pleistocene aquifer, that
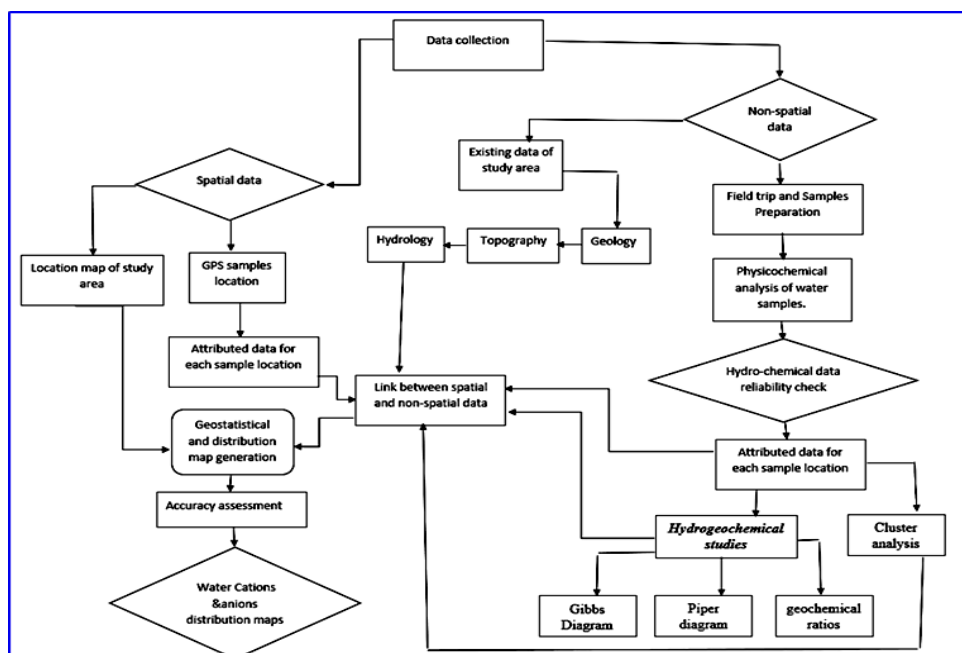

Figure (1): Flow chart showing the methodology adopted for groundwater quality mapping.

comprises of gravel, sand, and clay, is regarded the secondary aquifer in the study region. It is exposed at the outer edges of the Nile aquifer system adjoining the floodplain.

Data used

Water quality and Samples collection

The water quality for the research region was reported during a field trip on May 20-25, 2021. The goal of this trip was to document some field observations and administer a questionnaire on water quality in several rural villages within the study area. Meanwhile, on August 18-30, 2021, a second field trip was conducted to collect 79 water samples from various resources, including surface, shallow, and ground wells, as follows: 29 surface, 25 shallow, and 24 groundwater samples. All water samples were collected in two liter high-density polyethylene bottles that were acid-treated and thoroughly rinsed with de-ionized water before use, dried, and stored with the caps on to avoid contamination.

To prevent as much change in the composition of water as possible, collected samples were maintained at a temperature of roughly 4°C in ice-boxes until they arrived at the laboratory. Surface water samples were obtained at 0.5 m depths, shallow samples at 6 to 21 m depths, and groundwater samples at 45 to 82 m depths. The coordination of the 79 water samples tested was identified using a handheld GPS instrument, the GARMIN GPS 12 CX (Figure 3). During the field trip, water temperature (T ^{o}C) was measured *in situ* at the sampling sites using a mercury thermometer ranging from 0 to 100 Celsius degrees (°C). To acidify water samples (pH 1.5-2.0) for metal detection, concentrated HNO_3 was employed. Water samples were analyzed just after arrival at the laboratory within twenty-four hours of collection.
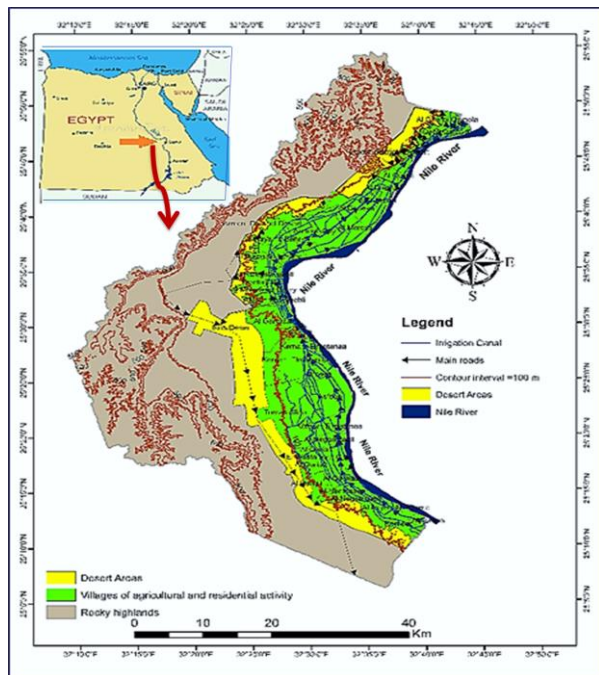

Figure (2): Location map with topography features of the study area extracted from Landsat-8 image.
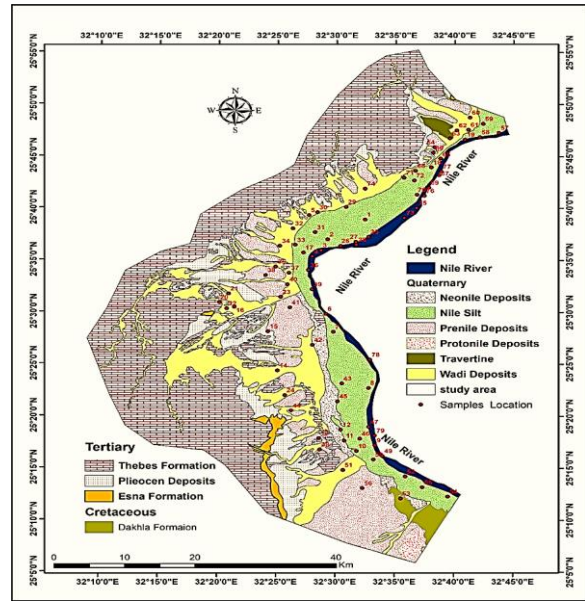

Figure (3): Geological map of the study area, with water sample locations, digitised from Map (CONOCO 1987).

Physicochemical analysis of water samples

The analysis processes were carried out in a water and air lab. in the central laboratory of the Egyptian Mineral Resources Authority (EMRA) with the assistance of the staff of the laboratory (Baird and Bridgewater, 2017). Physical parameters of the collected water samples were measured.

Electrical Conductivity (EC)

EC was measured by an electric conductivity meter model YSI 33, the U.S. with an accuracy of ±1%.

Total Dissolved Solids (TDS)

TDS were detected by evaporated known volume of sample water till dryness at 180 ^{o}C.

Chemical parameters

Chemical water analysis were determined including: pH that measured by a pH meter (WTW-Multilane, Germany, with an accuracy of ±1%), and major cations; Calcium (Ca^{2+}), and Magnesium (Mg^{2+}) were detected by volumetric analysis through titration against a standard EDTA solution (0.02 M) using Murexide (MX) and Eriochrome Black T (EBT) indicators at pH ≥ 12. Meanwhile, Sodium and Potassium were determined by atomic absorption spectrometry (Thermo fisher scientific, ICE 3000 SERIS). Major anions; Bicarbonate (HCO^-) and Carbonate (CO_3^{2-}) were determined volumetrically by the standard solution of sulfuric acid (0.02N) as a titrant with phenolphthalein and cresol green indicators. Chloride ion was determined by titrating 50 ml of water samples against 0.1N $AgNO_3^-$ using potassium chromate as an indicator while sulfate (SO_4^{2-}) was determined by partition gravimetric method through $BaSO_4$, the resulted turbidity was measured against standard solutions prepared under the same experimental conditions as water samples and was determined by spectro-photometer model UV-160A UV-Visible.

Moreover, nutrients such as NH_4^+ were analyzed by ammonia selective electrode (ISE Digital DM-21). NO_3^- and PO_4^{3-} were determined spectrophotometrically. The trace elements (Fe, Mn, Cu, Cd, Ni, Co, Pb, As) were determined using Inductive Coupling Plasma (I.C.P.) Agilent 720.
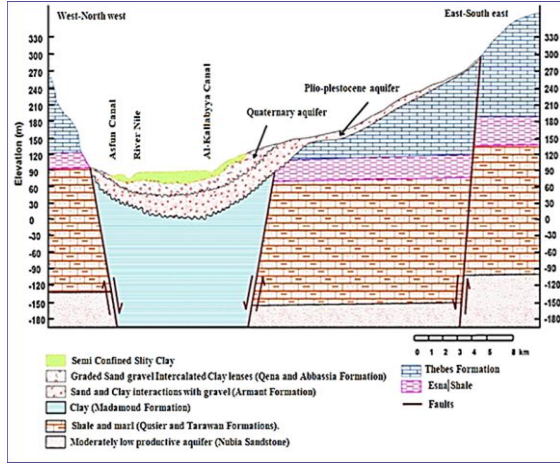

Figure (4): Hydrogeological cross-section at Luxor area (Ahmed and Fogg, 2014; Salman *et al.*, 2019).

Data processing, analysis and interpretation

Hydro-chemical data reliability check

The major cations (Na^+, Ca^{2+}, Mg^{2+}, K^+) and anions (HCO^-, CO_3^{2-}, Cl^-, SO_4^{2-}) concentrations in the different water bodies were displayed (Table 1). The accuracy of the laboratory-obtained data was examined using cations–anions balance. The solution must be electrically neutral (the sum of cations in meq/l should equal anions in meq/l) (Li *et al.*, 2018b; Yuan *et al.*, 2021) as shown in the following equation:

$$\text{Electro neutrality (\%)} = \frac{(\sum Cations - \sum Anions)}{(\sum Cations + \sum Anions)} \times 100$$

If the electrical balance calculates equal to or less than 5%, the analysis is good; if it is out of range (5%), the analysis is believed to be poor; this could be owing to the water being excessively acidic or certain constituents being missing during computation. However, up to 10% is permissible in dilute and saline water. The statistical approach of software excel Microsoft Office version 2019 and IBM statistical SPSS version 20 was used to obtain reliability.

Hydrogeochemical studies

The hydrogeochemical study includes water classifycation and graphical representation including the piper Diagram (Piper, 1944) by Aquachem version 4.0. (2010), computer software, and scatter or Gibbs Diagram (Gibbs, 1970). Gibbs's diagrams are used to reveal natural processes (evaporation, precipitation, and water-rock interaction) in different decades (Li *et al.*, 2016b). Piper plots are used to reveal the groundwater hydrochemical faces (Liu *et al.*, 2021).

Geostatistical analysis

Different techniques of geostatistical analysis were used through the Kriging method which is based on a weight mobile average that determines the extent of estimation error in each point in addition to estimated amounts. It is a linear interpolation procedure providing linear unbiased estimation for quantities, which vary in space and it is an advanced geo-statistical procedure that generates an estimated surface from a scattered set of points with z-values as follow:

$$Z\,(\boldsymbol{s_0}) = \sum\nolimits_{i=1}^{N} \lambda(S_i)$$

Where; Z(si) is measured value at the ith location; λi , is unknown weight for the measured value at the ith location; S0, is prediction location, and N, is number of measured values (Gundogdu and Guney 2007; Uyan and Cay 2013).

Statistical analysis

Correlation coefficients are used to measure how strong a relationship is between two variables by using IBM® SPSS® Statistics 20.0 software (2019).

RESULTS AND DISCUSSION

Reliability check for hydrochemical parameters of water samples indicates approximately 93.7 % of the measured water samples were within the range ($\leq$ 5%), thus results are ready for hydro-geochemical modeling. water samples' characteristics were displayed in Table (1).

General hydrogeochemical Analyses

The measured values of temperature for all water samples ranged between18 to 28 °C with an average of 22.5 °C indicating that shallow active water cycle or circulation is being limited to 100 or rarely 200 m (Pirzada, *et al.*, 2016). The variation of water T °C of water samples is due to water resource variety. pH values lie in the range of 6.45 to 8.69 with a mean value of 7.46; 26% of water samples have a pH of more than 8, and 39% have a range between 7-8, and 35% were less than 7. The alkalinity of surface water samples indicates increasing photosynthetic assimilation of dissolved inorganic carbon by plankton. On the other hand, most near shallow and groundwater samples indicate that most of the water bodies at the study area, are located on irrigation land water, flow-through limestone, and marl.

In addition, low pH values are due to clay and silt deposit at the quaternary aquifer (Qureshimatva, *et al.,* 2015), a geological map of the area is shown in Figure (3). The pH showed an indirect correlation with Ca^{2+} ions ($R^2 = -0.67$) which may be due to releasing of HCO_3^- ions from the Pliocene and Quaternary carbonate rocks. High values of TDS and EC for both shallow and deep groundwater indicated that 59% of the collected water samples belong to excessively mineralized water class >1000 µS/cm according to Al-Dahaan, *et al.* (2015) classification. Chebotraev's, (1955) classification for TDS values showed that water samples recorded 34% good potable, 6% fresh, 9% fairly fresh, 41% slightly brackish, 1% brackish and 9% slightly saline.

physicochemical parameters

Correlation coefficient matrix (R^2)

Physiochemical measurements revealed that there was correlation between TDS and water quality parameters as displayed in Table (2). It is clear that, there is linearly strong correlation between TDS versus Na (R= 0.990), Ca^{2+} (R= 0.920), Mg^{2+} (R= 0.930), SO_4^{2-} (R= 0.980) and Cl^- (R= 0.978), moderate correlation between TDS versus K^+ (R= 0.790) and HCO_3^- (R= 0.640). Finally, the correlation between TDS versus CO_3^{2-} (R= 0.010) is very weak. A strong correlation may be due to the dissolution of clay, silt, halite, gypsum, calcium carbonate, marl, and dolomite during the circulation of water. The value of NO_3^- and SO_4^{2-} gives a good indication of extensively anthropogenic activity and extensively usage of fertilizers during the agriculture process (Ahmed and Fogg, 2014).

GIBB'S Diagram

Gibbs' diagrams illustrate the distribution and correlation of total dissolved salt to dissolved ions in water samples lying in the zone of rock-water interaction dominance and evaporation rainfall dominance, revealing a mixed regulating mechanism (Figures 5A and B). The Chemicals weathering of rock-forming minerals will add the ions to the groundwater influencing the groundwater quality by the dissolution of rock through which water is circulating. Evaporation due to high temperature and absence of rainfall indicated the high ratios of dominant cations and anions, especially sodium ions, due to $CaCO_3$ precipitate caused by the combination of Ca^{2+} and HCO_3^- and extensively anthropogenic activities. Irrigation return flow elevated shallow and ground-water levels, hence increasing evaporation and inducing salinization (Gibbs, 1970; Wu *et al.*, 2015; Yuan *et al.*, 2019).

Chemistry of major cations-anions

The most domain cation is Na^+, and the other cations are in the following sequence ($Na^+>Ca^{2+} >Mg^{2+} >K^+$), as shown in Figure (6A). The high concentrations of Na^+, Ca^{2+}, and Mg^{2+} in water may be due to clay minerals such as Illite, Albite, Fluorite, Halite, Limestone, Dolomites, Gypsum, Sylvite, weathering of soda Feldspar (Albite), Potash Feldspars (Orthoclase and Microcline), and anthropogenic activities. Agriculture may supply Na^+ and K^+ ions to water through dissolution by carbonic acid, which is created by CO_2 existing in the soil zone due to weathering of parent materials or decomposing organic matter. CO_2 then mixes with water to form carbonates (Krishnaraj, *et al.*, 2011). Another source such as rainwater is slightly acidic due to the reaction with carbon dioxide in the atmosphere (Chen *et al.*, 2019b; Xu *et al.*, 2019).

Chloride is the most dominant anion, and the rest of the tested anions were in the following orders: ($Cl^-> SO_4^{2-}> HCO_3>CO_3^{2-}$) as shown in Figure (6B). Bicarbonate (HCO_3^-) and Carbonate (CO_3^{2-}) anions are formed by the reaction of carbon dioxide with water,

dissolution of carbonic acid (H_2CO_3), and carbonate rocks such as limestone and dolomite (Kojima *et al.*, 1997), in addition to weathering of clay rocks. The natural process such as weathering, dissolution of salt deposits as evaporation in the study area, weathering of sulfate and gypsum-bearing sedimentary rocks, and irrigation drainage return flow are responsible for Cl^- and SO_4^{2-} contents in addition to anthropogenic activity. The heavy use of agricultural fertilizers leads to increased chlorides in groundwater (Mostafa *et al.*, 2017; Li *et al.*, 2018b; Xu *et al.*, 2019; Zhang *et al.*, 2020).
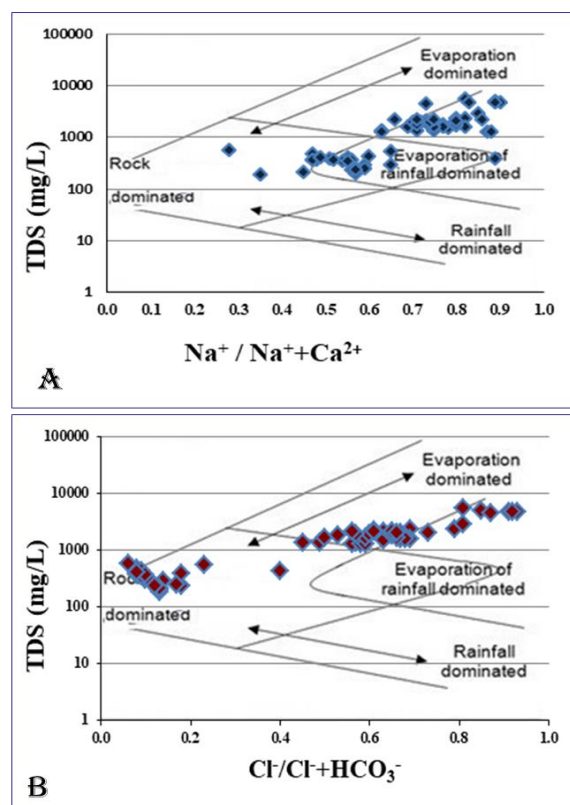

Figure 5: Gibbs' Diagrams showing total dissolved salts in correlation to dissolved ions. A, TDS verses to ratio of Na^+/Na^++Ca^{2+}; B, TDS verses to ration of Cl^-/ Cl+HCO_3^-

Hydrochemical facies

The method of Piper's trilinear diagram is considered a successful tool to classify different water sources by detecting hydrochemical facies types and natural processes (evaporation, water-rock interaction, and precipitation). From the cationic and anionic triangular files of the Piper diagram (Figure 7), it was observed that the majority of the samples fall into (Na+K) field in cations facies while 76% and 24 % of water samples fall into the Cl and no dominant fields in anion facies. By clustering 79 hydrochemical data based on anions, eight groups and fourteen subgroups of water type were detected (Table 3).

The table contains G1 Sodium (Chloride-Sulfate), G2 Sodium (Chloride-Bicarbonate), G3 Sodium (Bicarbonate-Chloride), G4 Sodium (bicarbonate-sulfate), G5 Calcium (bicarbonate-sulfate), G6 Sod-

Table (1): Physicochemical properties of different water samples collected from the Luxor area. For surface water (SW), shallow water (SH.W), and ground water, the minimal, maximum, and average values were estimated (GW).

Quality Parameter	Measured Parameters	Measured values								
		Minimum			Maximum			Average		
		SW	SH.W	GW	SW	SH.W	GW	SW	SH.W	GW
Physical	pH	6.59	6.45	6.53	8.54	8.53	8.59	7.78	7.15	7.35
	T °C	26.00	18.00	18.00	28.00	23.00	21.00	26.50	20.80	18.90
	TDS (mg/l)	183.4	374.94	1502.59	633.92	4445.93	5374.45	366.1	1600.89	2688.8
	EC (µS/cm)	265.89	598.32	2370.56	1103.34	714521	8945.45	608.28	2526.64	4213.97
Chemical	Na^+(mg/l)	13.87	58.45	350.74	71.78	1065.2	1421.64	39.80	346.43	689.93
	K^+(mg/l)	4.24	3.46	6.52	9.34	10.54	22.43	6.31	6.06	11.68
	Ca^{2+}(mg/l)	17.93	12.16	90.65	85.71	398.72	310.46	39.32	124.25	152.43
	Mg^{2+}(mg/l)	6.73	4.27	32.59	27.53	99.43	133.82	15.38	50.57	65.51
	CO_3^-(mg/l)	3.51	8.56	9.54	24.23	49.23	16.63	12.5217	15.99	13.07
	HCO_3^- (mg/l)	89.24	92.38	137.41	321.23	450.34	392.34	188.62	291.54	271.3
	SO_4^{2-} (mg/l)	15.94	30.35	296.63	56.46	291.54	1502.5	36.483	318.82	593.77
	Cl^- (mg/l)	11.62	36.25	427.52	47.56	1494.64	1721.56	19.84	429.152	863.35
	NH_4^+(mg/l)	0.01	0.7	0.12	3.20	4.30	3.4	1.5703	2.85	1.71
	NO_3^- (mg/l)	0.03	0.8	12.12	11.00	21.00	32	1.7431	10.95	23.52
	PO_4^{3-} (mg/l)	0.01	0.03	0.04	0.41	0.56	0.61	0.068	0.1744	0.3108
	Reliability check	1.07	1.39	1.075	5.94	5.98	5.46	2.96	2.86	2.31

Table (2): Correlation coefficient matrix of physicochemical parameters for the Luxor area

Parameter measured	TDS	EC	pH	Na^+	K^+	Ca^{2+}	Mg^{+2}	CO_3^{2-}	HCO_3^-	SO_4^{2-}	Cl^-
TDS	1										
EC	0.995	1									
pH	-0.55	-0.554	1								
Na^+	0.99	0.988	-0.491	1							
K^+	0.79	0.765	-0.349	0.787	1						
Ca^{2+}	0.92	0.918	-0.672	0.874	0.728	1					
Mg^{+2}	0.93	0.924	-0.584	0.891	0.747	0.882	1				
CO_3^{2-}	0.01	0.021	-0.454	-0.015	-0.162	0.097	0.03	1			
HCO_3^-	0.64	0.639	-0.909	0.574	0.355	0.763	0.672	0.472	1		
SO_4^{2-}	0.98	0.981	-0.439	0.989	0.802	0.851	0.877	-0.078	0.504	1	
Cl^-	0.978	0.986	-0.52	0.987	0.802	0.919	0.932	-0.021	0.612	0.967	1

Table (3): Water-type at Luxor area based on anions classification.

Classified Groups	Anions	Cations	Water type	Dominance Ions	Sample No.
G1	Cl^- SO_4^{2-}	Na^+ Ca^{2+}	Na-Cl- SO_4	Na>Ca>Mg>K $Cl>SO_4>HCO_3>CO_3$	5, 13, 14, 15, 16, 20, 21, 22, 23, 24, 33, 34, 35, 37, 38, 40, 41, 42, 44, 45, 48, 51, 56, 59, 60, 61, 62, 63, 64, 66, 68, 69, 71, 73 and 74
G2	Cl^- HCO_3^-	Na^+ Ca^{2+}	Na - Cl- HCO_3	Na>Ca>Mg>K $Cl>HCO_3>SO_4>CO_3$	25, 26, 29, 30, 31, 32, 53 and 57
G3	HCO_3^-,Cl^-	Na^+ Ca^{2+}	Na - HCO_3- Cl	Na>Ca>Mg>K $HCO_3>Cl>SO_4>CO_3$	6,8,11 and 21
G4	HCO_3^- SO_4^{2-}	Na^+ Ca^{2+}	Na- HCO_3-SO_4	Na>Ca>Mg>K $HCO_3>SO_4> Cl>CO_3$	1, 4, 7, 10, 12, 28, 36, 46, 47, 49, 50, 52, 55, 67,76 and 77
G5	HCO_3^- SO_4^{2-}	Ca^{2+} Na^+	Ca-Na- HCO_3- SO_4	Ca> Na>Mg>K $HCO_3>SO4>Cl> CO_3$	2, 17, 18, 19, 27, 39, 54, 58, 65, 70, 72, 75, 78 and 79
G6	SO_4^{2-} $·HCO_3^-$	Na^+	Na--SO_4-HCO_3	Na>Ca>Mg>K $SO_4>HCO_3>Cl> CO_3$	3
G7	Cl^-,SO_4^{2-} HCO_3	Na^+	Na-SO_4 -Cl	Na>Ca>Mg>K $SO_4>Cl>HCO_3> CO_3$	43

ium (sulfate- bicarbonate) and finally G7 Sodium (sulfate-chloride) water type. Water types hydrochemistry (Table 3) controlled by dissolution and leaching processes of evaporite deposits in clay minerals, higher levels of HCO_3^- concentrations compared to chloride and sulfate in most water samples infers mineral dissolution in addition to excessive fertilizer as a result of extensive irrigation and anthropogenic activity at Luxor area.
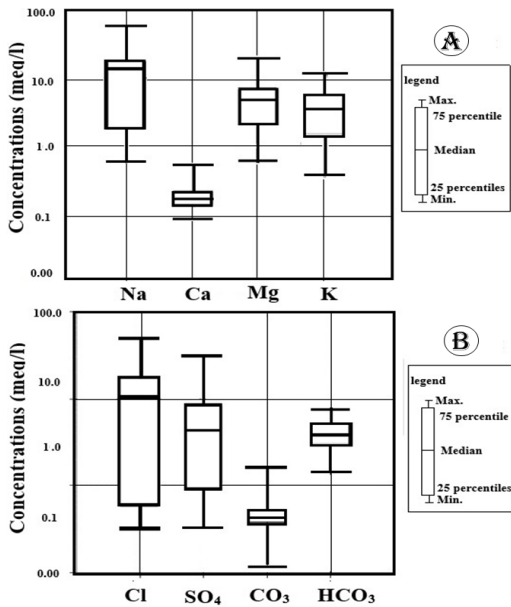

Figure (6): Box plots of major ion concentrations in the studied water samples at the Luxor area. A, Cation; B, anion.

Cluster analysis

The classification was achieved by (HCA) based on similarity and euclidian geometric distance among observations using Ward's method as the linkage rule. A total number of 19 water quality parameters are clustering as follows: [TDS, EC, pH, T°C, Na^+, Ca^{2+}, Mg^{2+}, k^+, CO_3^{2-}, HCO_3^-, SO_4^{2-}, Cl^-, PO_4^-, NH_4^+, NO_3^-, Fe, Mn, and Pb]. The results as a dendrogram (Figure 8) depend on visual exam-ination where there are two clusters group for physicochemical parameters. Cluster 1 included EC and TDS, while cluster 2 was separated into two subgroups which were divided into other subgroups. SG1 (3 Parameters are included; Na^+, SO_4^{2-}, Cl^-), SG2 was divided into [a- SSG2-1 (12 parameters are included; WD,T °C, pH, k^+, CO_3^{2-}, Ca^{2+}, PO_4^-, NH_4^+, NO_3^-, Fe, Mn and Pb), b- SSG2-2 (2 parameters; HCO_3^- and Mg^{2+})]. SG2 may be explained by combining mixed sources while the other elucidation dissolution of these minerals was conducted under slightly basic to basic conditions. SG1, including Na, SO_4, and Cl^-, since Na especially results from cations exchange while SO_4 and Cl have resulted from leaching of fertilizers from the soil horizon to the aquifer and it reflected the influence of domestic and agricultural pollution. Other HCA, which rendered 79 sampling sites into two statistically significant clusters at the sites, categorized into individual clusters that behave similarly and/or have a

similar origin. The first cluster (G1) comprises 33 sampling sites and the second cluster (G2) contains 46 sites which are divided into two subgroups SG 2-1 (6 samples) and SG 2-2 (40 samples), SG 2-1 divided into two other subgroups SSG 2-2-1 (22 samples) and SSG 2-2-2 (18 samples) as displayed in Figure (9).

Group 1 is characterized by TDS that ranged from 183.4 to 633.92 mg/l, high bicarbonate, sulfate, and low chloride concentration with Na-Ca-Mg-HCO_3 water type. The relatively low concentration of TDS is indicative of short residence time. All water samples of this group are characterized by surface water type. Sub-group 2-1 is characterized by TDS values from of
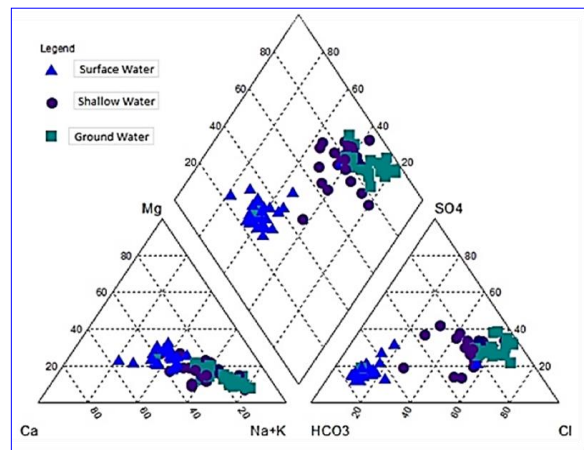

Figure (7): Water-type classification of water samples at the Luxor area.

4445.93 to 5374.45 mg/l, high chloride, sulfate, and bicarbonate concentrations with Na-Cl-SO_4 water type. The high concentration of TDS is indicative of long residence time, and high concentrations of sulfate and chloride are indicative of pollution. Most water samples of this group are specific for groundwater samples. Sub-Sub Sub-groups 2-2-1 is characterized by TDS values from 1875.05 to 2857.88 mg/l, high chloride, sulfate, and bicarbonate concentrations with Na-Ca-Cl-SO_4 water type. A high concentration of TDS is indic-ative of long residence time, and very high concentrations of sulfate and chloride are indicative of pollution. Most of the water samples of this group are characterized by groundwater samples. Sub-Sub groups 2-2-2 are characterized by TDS values from 3940 to 6112 mg/l, very high chloride, sulfate, and low bicarbonate concentration with Na-Ca-Cl-SO_4-HCO_3 water type. The high concentration of TDS is indicative of long residence time with contact with soluble minerals such as limestone, marl, silts, evaporates deposits, and clay. Very high concen-trations of sulfate and chloride are indicative of high pollution from extensive use of fertilizer with anthropogenic activity. Most of the water samples of this group are characterized by shallow samples.

Geo-statistical analysis

The prediction maps for hydrochemical parameters are created by changing parameters of the Kriging method to estimate the spatial variation of
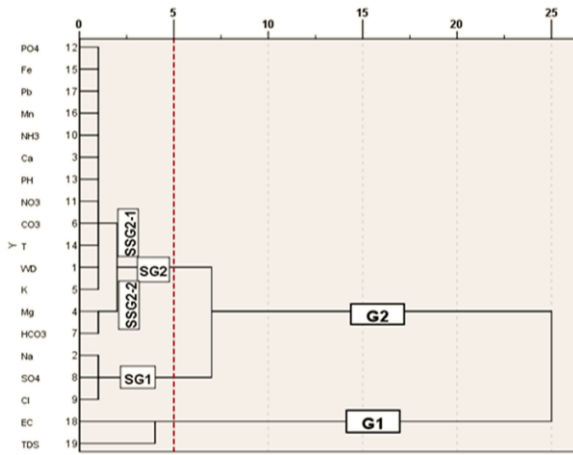
Figure (8): Dendrogram for cluster analysis of water parameters.
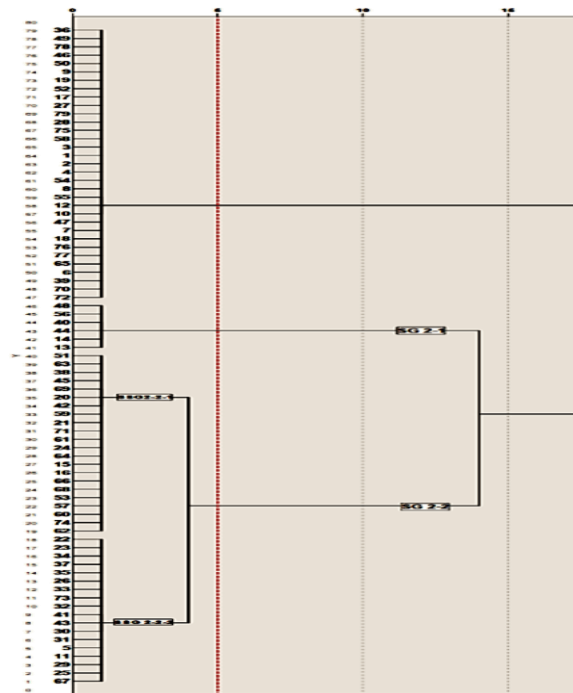

Figure (9): Dendrogram for cluster analysis of classified water samples.

hydrochemical parameters with achieving the principle that the mean errors and root-mean-square errors are close to 0 and 1, or lower values as possible. The prediction kriging maps for distributing pH, water deep (WD), major cations, and anions of water bodies at the Luxor area are shown in (Figures 10, 11, 12, and 13). The geostatistical prediction results indicated the hydrochemical parameters are generally increasing in concentration from east to west, where groundwater and shallow water have high salts content (Ayman *et al.*, 2013; Masoud *et al.*, 2010; Salman *et al.*, 2019). A deep prediction map indicates the level of groundwater increased systemically from the east to west and the deep increase as far from the quaternary aquifer. This result matched with that obtained for the topography and geology of the study area (Figures 2 and 3). The distribution of pH values indicates no standard interpretation for a geological process that means a primary indication of pollution sources. This may be due to

extensive use of fertilizer or mixed with human pollution from sewage systems.

Prediction maps of TDS and EC indicated that deepwater has high salt content over-irrigation area. Prediction maps at Esna indicated a high concentration of TDS and EC with salt content (Na^+, Cl^- and SO_4^{2-}) which is in agreement with the aquifer formation of Esna which comprises highly permeable sand and gravel with variable thickness and a semi-confining layer consisting of clay and silt. Recharge components include the deep percolation of irrigation surplus and seepage losses from irrigation canals. Prediction maps indicate a high concentration of Na^+, Cl^- and SO_4^{2-} at new reclamation land that showed an external source of these chemical constituents which may be using chemical fertilizers.

Water sample tests found a high percent of HCO_3^- and CO_3^{2-} concentrations spatially in Luxor and Esna. This is owing to the presence of urban settlements, various services in tourist locations, and floating hotels on the western bank of Luxor and Esna. These factors contribute to increased photosynthetic absorption of dissolved inorganic carbon by plankton.

Heavy metals

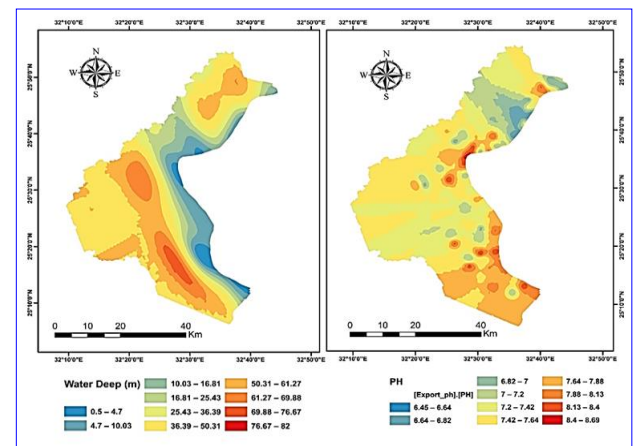Heavy metals exist throughout the earth's crust as naturally occurring elements. Anthropogenic activities

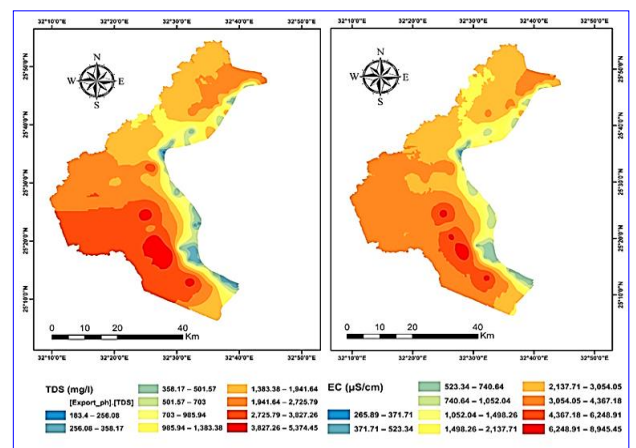**Figure (10):** Prediction maps of WD and pH of water bodies at Luxor area.

Figure (11): Prediction maps of (EC) and TDS of water bodies in the Luxor area.
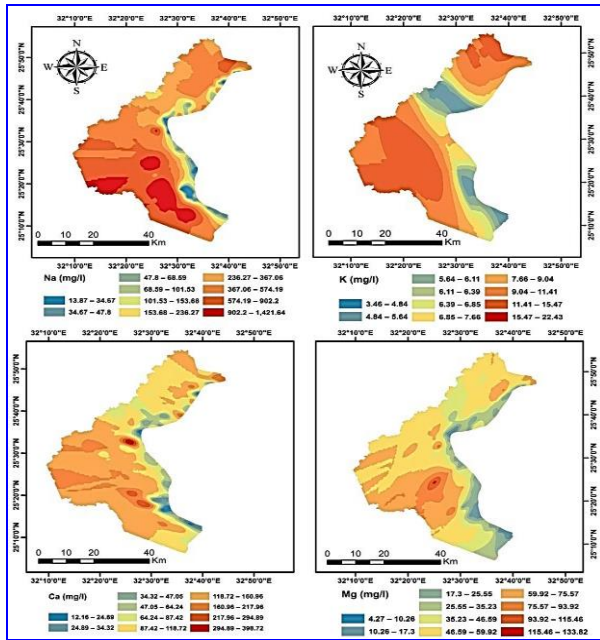
Figure (12): Prediction maps of major cations of water bodies in the Luxor area.
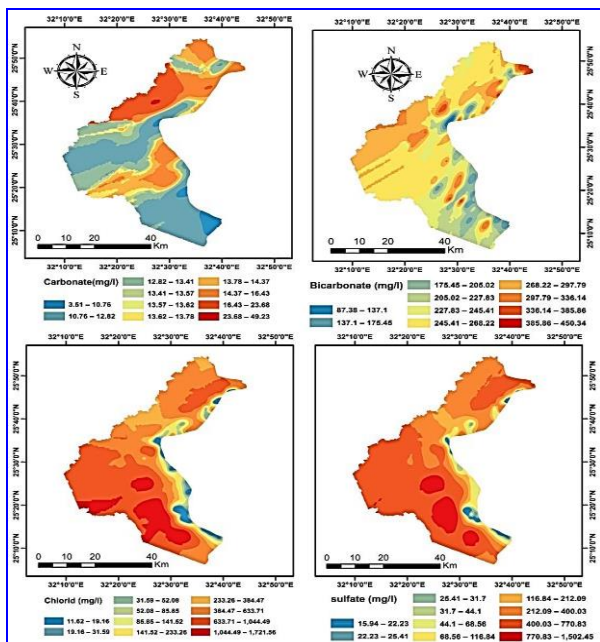

Figure (13): Prediction maps of major anions of water bodies in the Luxor area.

such as industrial production, mining and smelting operations, domestic and agricultural use of metals, and metal-containing compounds result in most environmental contamination and human exposure (Bradl, 2004). As clear from Table (5) it was found that most of the examined water samples have high levels of (Fe, Mn, Cd, Ni, Co, and As) in some locations according to Egyptian Standard Limits Law No. 458 (EMH, 2007), indicating contamination of water with industrial, mining, domestic and agriculture fertilizers, accredited to anthropogenic activities (tourist activities in Luxor and Esna, factories, sugar factory of Arment city), as well as natural processes (such as changes in precipitation inputs, erosion, weathering of Paleocene-Eocene, Pliocene, and

Pleistocene-Holocene rocks). These results were similar to those reported (El Tahlawi et al., 2016; El-Aassar *et al.,* 2016; Asmoay, 2017; Salman *et al.,* 2017; Salman *et al.,* 2019) who concluded that the pollution of water forms at the study area with these metals could be related to the widespread tender of P-fertilizers, which contain extensive concentrations of Cd and Pb. Mn and Co are present in the ferroma-gnesian minerals in the sediments of the west Luxor.

Nutrients

As shown in Table (1), the recorded concentrations of nutrients (NH_4^+, NO_3^-, PO_4^{3-}) were within the permissible level (EMH, 2007). The prediction kriging maps for nutrients of water bodies at the study area were displayed (Figure 14).
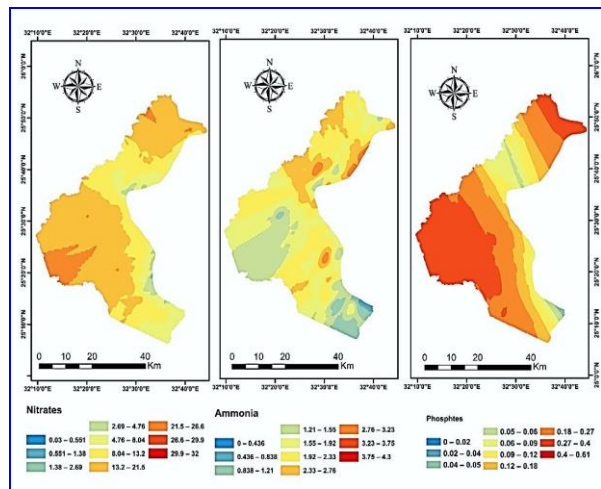

Figure (14): Prediction maps of nutrients for the collected water samples in the Luxor area.

CONCLUSION

It can be concluded that according to the Piper diagram, dominant hydrogeochemical facies of water bodies showed that the Na-Cl type covers large parts of the eastern and central sides of the Luxor area and changed to the Na-Cl-HCO$_3$ and Na-Cl-SO$_4$ types in the shallow water. Surface water has a mixed type of Na-Ca-Mg-HCO$_3$. The Gibbs plot indicated that the hydrochemistry of water in the Luxor area was mainly controlled by the weathering of minerals and evaporation. The excessive sodium concentration may be due to the mixed mechanism of weathering of silicate rocks, and evaporation which leads to CaCO$_3$ precipitate caused by the combination of Ca^{2+}and HCO$_3^-$ in addition to ion exchange between calcium and sodium of clay minerals. High concentrations of SO$_4^{2-}$ and Cl$^-$ may be due to huge quantities of irrigation water contaminated with fertilizer which lead to an increase in groundwater levels, hence increasing evaporation and inducing salinization. Based on the hierarchical cluster analysis, water samples were classified into two major groups (G1 and G2) and three subgroups (SG1-2, SSG2-2-1, and SSG2-2-2). Based on Piper classification**,** it was obser ved that these subgroups of water samples of Luxor fall in Na-Cl, Na-SO$_4$, mixed type with Na-HCO$_3$ and

Table (5): Concentration of heavy metals of the studied water samples of Luxor.

Measured Parameters	Measured values									ESL (2007)
	Minimum			Maximum			Average			
	S.W	SH.W	G.W	S.W	SH.W	G.W	S.W	SH.W	G.W	
Fe (mg/l)	0.01	0.01	0.02	0.91	0.81	0.85	0.24	0.3	0.34	0.3
Mn (mg/l)	0.1	0.26	0.12	0.86	0.78	1.20	0.33	0.48	0.53	0.4
Pb (mg/l)	0.06	0.12	0.01	0.47	0.56	0.24	0.30	0.30	0.05	0.01
Cd (mg/l)	0.01	0.01	0.01	0.03	0.03	0.10	0.016	0.01	0.04	0.003
Cu (mg/l)	0.1	0.1	0.13	0.25	0.27	0.13	0.18	0.14	0.13	2.00
Co (mg/l)	0.02	0.05	0.07	0.32	0.32	0.16	0.15	0.16	0.11	0.04
Ni (mg/l)	0.02	0.01	0.01	0.33	0.26	0.16	0.17	0.12	0.05	0.02
As (mg/l)	0.9	1.10	0.02	4.21	3.20	0.51	2.25	1.75	0.15	0.01

$Ca-Mg-HCO_3$ water type. Geo-statistical techniques especially Kriging give a good illustration for the distribution of hydrochemical parameters of surface, shallow, and groundwater which agreed with the classical statistical hydro-geochemical analysis. Using the results of Kriging maps as the supportive method in inventing ways for making sustainable environmental management before setting up strategies can simplify the better prediction of water management. Spatial distribution maps showed that the Esna area has a higher value of TDS for shallow and deep water. The salinity was increasing from east to west of the Luxor area. Luxor and Esna city has a high value of bicarbonate due to extensive anthropogenic activities.

REFERENCES

ABD EL-BASSIER, M.A., 1997. Hydrogeological and hydrochemical studies of the Quaternary Aquifer in Qena Governorate, Egypt. (M.Sc. Thesis). Faculty of Science Assiut University, Egypt,163.

AL-OMRAN ABDULRASOUL M., ALY ANWAR A., AL-WABE MOHAMMAD I., AL -SHAYAA MOHAMMAD S., ABDULAZEAM SALLAM S., NADEEM MAHMOUD E., 2017, Geostatistical methods in evaluating spatial variability of groundwater quality in Al-Kharj Region, Saudi Arabia, Journal of Applied Water Sciences, 7:4663–4671.

ABOU HUSSEIN, S.D., SAWAN, O.M., 2010, The utilization of agricultural waste as one of the environmental issues in Egypt (a case study). Journal of Applied Sciences Research, 6(8):1116–1124.

AGARWAL, R., GARG, P., 2016. Remote Sensing and GIS-Based Groundwater Potential & Recharge Zones Mapping Using Multi-Criteria Decision Making Technique. Water Resources Management, 30: 243–260.

AHMED, A.A., FOGG, G.E., 2014. The impact of groundwater and agricultural expansion on the archaeological sites at Luxor, Egypt. Journal of African Earth Sciences,95:93–104.

AL-DAHAAN, S., ALABIDI, A., AL-ANSARI, N., KNUTSSON, S., 2015. Relationship between Selected Hydrochemical Parameters in springs of Najaf Province, Journal of Iraq. Engineering, 7(6): 337-346.

BAIRD, R., BRIDGEWATER, L. (2017). Standard methods for the examination of water and wastewater. 23rd edition. Washington, D.C.: American Public Health Association.

ASLAN, V., ÇELIK, R., 2021. Integrated GIS-Based Multi-Criteria, Analysis for Groundwater Potential Mapping in the Euphrates's Sub-Basin, Harran Basin, Turkey. Sustainability, 13(13):7375.

ASMOAY, A.S.A., 2017. Hydrogeochemical Studies on the Water Resources and Soil Characteristics in the Western Bank of the River Nile between Abu Qurqas and Dayr Mawas, El Minya Governorate, Egypt (Ph.D. Thesis). Faculty of Science, Al Azhar University, Egypt, 254.

AYMAN A. AHMED, GRAHAM E. FOGG, MOHSEN A. GAMEH, 2013: Water use at Luxor, Egypt: consumption analysis and future demand forecasting, Journal of Environmental Earth Science, 72:1041–1053.

BAO Z., WU, W., LIU, H., CHEN, H., YIN, S., 2014: Impact of long-term irrigation with sewage on heavy metals in soils, crops, and groundwater a case study in Beijing. Pol J Environ Stud 23 (2):309–318.

BELKHIRI, L., BOUDOUKHA, A., MOUNI, L., (2010), A multivariate Statistical Analysis of Groundwater Chemistry Data, International Journal of Environmental Research, 5(2): 537-544.

BRADL, H.B.,2004, Adsorption of heavy metal ions on soils and soils constituents. Journal of Colloid and Interface Science.277(1):1-18.

CHAI, H., CHENG, W., ZHOU, C., CHEN, X., MA, X., ZHAO, S., 2011. Analysis and comparison of spatial interpolation methods for temperature data Xinjiang Uygur Autonomous Region, China. Natural Science, 3(12):999–1010.

CHEBOTEREV, I., (1955). Metamorphism of natural

waters in the crust of weathering-I. Geochimica et Cosmochima Acta, 8(1-2): 22-48.

CHEN, J., HUANG, Q W., LIN, Y., FANG, Y., QIAN, H., LIU, R., MA, H., 2019b. Hydrogeochemical Characteristics and Quality Assessment of Groundwater in an Irrigated Region, Northwest China. Water, 11(1): 96.

CHEN, Q., J.C. WEI, C.P. JIA, H.M. WANG, L.Q. SHI, S.L. LIU, F.Z. NING, Y.H. JI, F.Y. DONG, AND Z.W. JIA. 2019b. Groundwater selenium level and its enrichment dynamics in seawater intrusion area along the northern coastal zones of Shandong Province, China. Geochemistry International 57(11), 1235– 1241.

CONOCO, (1987). Geological Map of Egypt, Scale 1: 500,000, NG 36 SW Luxor. The Egyptian General Petroleum Corporation, Cairo (EGPC), Egypt.

ÇELIK, R., 2019, Evaluation of groundwater potential by GIS-based multicriteria decision making as a spatial prediction tool: a case study in the Tigris River Batman-Hasankeyf sub-basin, Turkey, Water, 11 (12): 2630

DEEPESH MACHIWALA, MADAN K. JHAB, 2015. Identifying sources of groundwater contamination in a hard-rock aquifer system using multivariate statistical analyses and GIS-based geostatistical modeling techniques, Journal of Hydrology: Regional Studies 4: 80–110.

EL ALFY, M., ALHARBI, T., MANSOUR, B., 2018. Integ-rating geochemical investigations and geospatial assessment to understand the evolutionary process of hydro-chemistry and groundwater quality in arid areas, Environ. Monit. Assess. 190 (5): 277.

EL TAHLAWI, M.R.; ABO-EL KASSEM, M.; BAGHDADI, G.Y.; SALEEM, H.A., (2016). Assessment of groundwater vulnerability, a case study. International Journal of Advanced Remote Sensing and GIS,5 (2): 1561–1579.

EL-AASSAR, E.M., HUSSIEN, R.A., GHOUBACHI, S.Y., 2016. Groundwater quality and vulnerability asses-sment in the new reclamation areas, Assuit governorate, West Nile River, Egypt. Journal of American Sciences, 12(11):1-23.

EMH (2007). Ministerial decree (# 458/2007) on guidelines for drinking water quality and the water quality for household uses. Egyptian Ministry of Health, Cairo

GIBBS, R. J., 1970. Mechanisms controlling world water chemistry. Science, 170 (3962): 1088–1090.

GUNARATHNA, M.H.J.P., KUMARI, M.K.N., NIRMANEE K.G.S., 2016. Evaluation of Interpolation Methods for mapping pH of Groundwater, IJLTEMAS.4 (3): 1-5.

GUNDOGDU, K.S., AND GUNEY, I., 2007, Spatial Analyses of Groundwater Levels Using Universal Kriging. Journal of Earth System Science, 116: 49-55.

HONGYING YUAN, SHUQING YANG, B.,O WANG , TIANKAI HAN, XUEHUA DING, 2021. Hydro-Geochemical Characteristics and Quality Evaluations of the Groundwater of an Irrigated

Plain Region of Northwestern China, research square,1:1-22

JAMIL SIDDIQUE ,JIN MENGGUI ,MUNIR H. SHAH, ASFANDYAR SHAHAB, FAISAL REHMAN, UMAIR RASOOL, 2020. Integrated Approach to Hydrogeochemical Appraisal and Quality Assessment of Groundwater from Sargodha District, Pakistan, Geofluids, 2020:(1-15)

KAMEL, E.R., 2004. Geology of Luxor area and its relationship to groundwater uprising under the Pharaoh's Temples. M. Sc. Thesis, Aswan Faculty of Science, South Valley University, Egypt.

KOJIMA, T., NAGAMINE, A., UENO, N., UEMIYA, S., 1997, Absorption and fixation of carbon dioxide by rock weathering, Energy Conversion, and Management, 38(5):461- 466.

KRISHNARAJ, R., MURUGESAN,V., VIJAYAR-AGHAVAN, K., SABARATHINAM,C., PALU-CHAMY, A., RAMACHANDRAN, M., 2011, Use of Hydrochemistry and Stable Isotopes as Tools for Groundwater Evolution and Contam-ination Invest-igations, Journal of Geosciences 1(1): 16-25

LI, P ., WU, J., TIAN, R., HE, S., HE, X., XUE, C., ZHANG, K., 2018b. Geochemistry, Hydraulic Connectivity and Quality Appraisal of Multilayered Groundwater in the Hongdunzi Coal Mine, Northwest China. Mine Water Environ., 37: 222–237.

LI, P., WU, J., QIAN, H., ZHANG, Y., YANG, N., JING, L., Yu, P., 2016b. Hydrogeochemical characterization of groundwater in and around a wastewater irrigated forest in the southeastern edge of the Tengger Desert, Northwest China. Journal of Exposure and Health, 8: 331–348.

LIU, X., XIANG, W., SI, B.C., 2021. Hydrochemical and isotope characteristics in the shallow groundwater of the Fenhe River basin and indicative significance, Journal of Environmental Science, 42(4):1739-1749

LOSSER,T., LI, L., PILTNER, R.A., 2014. Spatiot-emporal interpolation method using radial basis functions for geo-spatiotemporal big data. In: 5th International Conference on Computing for Geospatial Research and Application, 17–24.

MAHATO, M.K., SINGH, P.K., TIWARI, A.K., 2016. Hydrogeochemical evaluation of groundwater quality and seasonal variation in East Bokaro Coalfield Region, Jharkhand. Journal of the Geological Society of India 88:173–184.

AHMADIAN, M., CHAVOSHIAN, M., 2012. Spatial Variability Zonation of Groundwater-table by Use Geostatistical Methods in Central Region of Hamadan province, Scholars Research Library, Annals of Biological Research, 3 (11):5304-5312.

MASOUD, A.M., ABDEL-MONEIM, A.A, AYMAN, A., YOUSSEF, A.M., 2010. Evaluation of Hydrogeological Conditions in the desert area west of Armant, Upper Egypt, The 4th International Conference on Healthy Water in Arab World (Water for Healthy Arab Citizens), 21–22 June 2010, Semiramis Intercontinental, Cairo, Egypt, Corniche El Nil, Cairo, Egypt, Arab Healthy Water Association.

MOSTAFA M.G., HELAL S.M., HAQUE A.B., 2017. Assessment of hydro-geochemistry and groundwater quality of Rajshahi City in Bangladesh, Applied Water Science 7: 4663–4671.

PIPER, A., 1944. A graphic procedure in the geochemical interpretation of water analyses. Transactions, American Geophysical Union. 25 (6): 914-928.

QURESHIMATVA, U.M., MAURYA, R.R., GAMIT, S.B., PATEL, R.D., SOLANKI, H.A., 2015. Determination of Physico-Chemical Parameters and Water Quality Index (Wqi) of Chandlodia Lake, Ahmedabad, Gujarat, India. Journal of Environmental & Analytical Toxicology,5(4):1-6

SABRY A. ABDALLAH, HASSAN R. EL-RAMADY, ABDELHAKEEM E. EL-SHERBENI, HELMY A. ANBER, ELSAYED A. KISHK, SOBHY HAMED, AND HAZEM M. AMINE 2019. Monitoring Water Quality of Some Canals in Delta Region, Egypt, Environment, Biodiversity and Soil Security 3(5): 73 – 95.

SAID, R., 1981. The geological evolution of the River Nile. Springer, New York Inc, 151.

SALMAN A. SALMAN, MERCEDES ARAUZO, AHMED A. ELNAZER, 2019. Groundwater quality and vulnerability assessment in west Luxor Governorate, Egypt, Groundwater for Sustainable Development, 8: 271–280

SALMAN, S.A., ELNAZER, A.A., EL NAZER, H.A., 2017. Integrated mass balance of some heavy metals fluxes in Yaakob village, south Sohag, Egypt. International Journal of Environmental Sciences &Technology 14(5):1011–1018.

PIRZADA TAJNEES , MIR MUNSIF, ALI TALPUR, AZIZA AFTAB, MARIA KALEEMAND, BUSHRA SHAHAB. 2016. Hydrochemical Analysis and Evaluation of Groundwater Quality and Agriculture Soil of Khairpur Taluka, Sindh, Pakistan, Pak. Journal of Analytical & Environmental Chemistry.17 (1): 23-32.

TRIKI, I., TRABELSI, N., HENTATI, I., ZAIRI, M., 2013: Groundwater levels time series sensitivity to pluviometry and air temperature: a geostatistical approach to Sfax region, Tunisia. Environ Monitoring and Assessment 186(3):1593–1608.

RYAN, M., CAY, T., 2013. Spatial analyses of ground-water level differences using geostatistical mod-eling. Journal of Environmental and Ecological Statistics 20 (4):633–646.

WU, J., LI, P ., QIAN, H., 2015. Hydrochemical characterization of drinking groundwater with special reference to fluoride in an arid area of China and the control of aquifer leakage on its concentrations. Journal of Environmental Earth Sciences, 73(12): 8575–8588.

WU, J., LI, P., QIAN, H., DUAN, Z., ZHANG, X., 2014. Using correlation and multivariate statistical analysis to identify hydrogeochemical processes affecting the major ion chemistry of waters: A case study in Laoheba phosphorite mine in Sichuan, China. Arabian Journal of Geosciences, 7(10): 3973– 3982.

XU, P.P., FENG, W.W.; QIAN, H.; ZHANG Q.Y., (2019). Hydrogeochemical Characterization and Irrigation Quality Assessment of Shallow Groundwater in the Central-Western Guanzhong Basin, China[J]. International Journal of Environ-mental Research and Public Health,16(9):1492.

YANG, Q., WANG, L., MA, H., YU, K., MARTÍN, J.D., 2016. Hydrochemical characterization and pollution sources identification of groundwater in Salawusu aquifer system of Ordos Basin, China. Environ. Pollut. 216(9): 340–349.

XIAO, Y., GU, X., YIN, S., SHAO, J., CUI, Y., ZHANG, Q., & NIU, Y., 2016. Geostatistical interpolation model selection based on ArcGIS and Spatio-temporal variability analysis of groundwater level in piedmont plains, northwest China. Springer Plus, 5(425):1-15

YUAN, H.Y.,YANG, S.Q., DING, X. H., WANG, B.O., YANG, X.M., 2019. Evolution characteristics of nutrients and chemical compositions of groundwater before and after autumn irrigation-Taking Wulate Irrigation Area as an Example [J].Environmental Chemistry, 38(10):2336-2347.

ZANDI, S., GHOBAKHLOU, A., SALLIS, P., 2011.Evaluation of Spatial Interpolation Techniques for Mapping Soil pH, 19th International Congress on Modelling and Simulation, Perth, Australia, 12–16 December 2011, 1153-1159.

ZHANG, T., HE, J., LI, J.J., CAO, Y.T., GONG, L., LIU, J.W., BIAN, C., CAI, Y.M., 2018. Major ionic features and possible controls in the groundwater in the Hamatong River Basin[J]. Environmental Science, 39(11): 4981-4989.

ZHANG, W., WANG, D.W., LEI, K., LV, X.B., CHEN, Y., YANG, L.B., 2020. Hydrochemical characteristics and impact factors in the middle and lower reaches of the Yellow River in the wet season [J]. Research of Soil and Water Conservation, 27(1): 380-386.

التحقيق الهيدروجيوكيميائي لموارد المياه السطحية والجوفية في منطقة غرب الأقصر، مصر بإستخدام التقنيات المكانية والإحصائية

مرفت السنباطى[1]، مى الجمال[1]، احمد الزينى[2]، محمد جبريل[3]

[1] قسم العلوم البيئية، كلية العلوم، جامعة دمياط، دمياط، مصر
[2] قسم الدراسات البيئية ،الهيئة القومية للأستشعارمن بعد وعلوم الفضاء،القاهرة، مصر
[3] قسم الدراسات الجيوكيميائية ،المعامل المركزية، الهيئة المصرية العامة للثروة المعدنية، الجيزة، مصر

الملخص العربــي

أدى زيادة الإستخدام لمصادرالمياة وممارسات إداراة الأراضى فى منطقة غرب الأقصر الى تدهور نوعية المياة وامكانياتها. لذلك هدفت الدراسة الحالية الى مراقبة العمليات الهيدروجيوكيميائية للموارد المائية بمنطقة غرب الأقصر- مصر. تم جمع 79 عينة من مختلف مصادر المياة بمنطقة الدراسة والمتمثلة فى المياة السطحية والضحلة والجوفية فى الفترة اغسطس 2021م. تم استخدام ثلاث طرق تحليلية احصائية فى هذة الدراسة تتمثل فى التحليل الهيدروجيوكيميائى الإحصائى الكلاسيكى والتحليل الإحصائى العنقودى والتحليل الإحصائى المكانى. تم رسم خرائط خصائص المياة بأستخدام طريقة كريجنج كأداة جيواحصائية من ادوات برنامج ارك ماب 10.4.1. وأظهرت النتائج المختبرية التكامل بين مخطط باير والتحليل الهيدروجيوكيميائى العنقودى وخرائط التنبؤ الجيواحصائى. كما اظهرت النتائج هيمنة شوارد الكاتيونات بالترتيب الآتى ($Na^+ > Ca^{2+} > Mg^{2+} > K^+$) وهيمنة شوارد الأنيونات بالترتيب الآتى ($Cl^- > SO_4^{2-} > HCO_3^- > CO_3^{2-}$). تبين من النتائج ان سحنات المياه الشائعة من النوع (Na-Cl) والأنواع المختلطة (-Na-Cl), (Na-Cl-HCO_3), (SO_4, Na-Ca-Mg-HCO_3). أظهرت نتائج التكامل بين خرائط التنبؤ والتحليل الإحصائى الهيدروجيوكيميائى الى ان عينات المياة الضحلة والجوفية أعلى من الحدود القياسية المصرية المسموح بها لجودة المياة لعام 2007 م لمحتوى الأملاح والمعادن الثقيلة (Fe, Mn, Co, Ni, Cd, Pb, As) فى حين ان المياة السطحية سجلت قيم مرتفعة من الرقم الهيدروجينى ونسب ال (HCO_3^-, CO_3^{2-}) مما يشير الى وجود مصادر لتلوث المياة . وهكذا، خلصت هذه الدراسة إلى أن التكامل بين التحليل الإحصائي الكلاسيكى و التحليل الإحصائى الهيدروجيوكيميائي العنقودى والتحليل الإحصائى المكانى قد أعطى تحقيقا جيدا لكل من عمليات المياه الطبيعية وكذلك نوعية المياه في منطقة غرب الأقصر.